Surgical and Radiologic Anatomy (2025) 47:188
https://doi.org/10.1007/s00276-025-03697-7

ORIGINAL ARTICLE

Radiological analysis of palatal arterial anatomy for periodontal surgery: insights from 3D-RA

Ahmet Aydogdu[1] · **Evrim Bozay Oz**[2] · **Ibrahim Ilker Oz**[3]

Received: 29 May 2025 / Accepted: 25 July 2025

Abstract

Objective This study aimed to comprehensively evaluate the detailed arterial anatomy of the palatal mucosa, emphasising the greater palatine artery (GPA) and lesser palatine artery (LPA), through the use of three-dimensional rotational angiography (3D-RA). This detailed vascular analysis aims to inform clinical decisions and reduce the risk of vascular injury during palatal graft harvesting procedures.

Methods A retrospective analysis of radiological data was conducted on 80 consecutive patients who underwent cerebral or carotid digital subtraction angiography (DSA) incorporating 3D-RA imaging. Detailed measurements were obtained for the GPA, descending palatine artery (DPA), and LPA, including arterial diameters, branching patterns, and their spatial relationships with palatal mucosal thickness and vault morphology. Based on GPA and LPA branching patterns, the vascular supply to the hard palate was classified.

Results The GPA was classified into three branching patterns, with Type I (absence of medial branch) being most prevalent (65%), typically accompanied by the presence of LPA contributions to the medial hard palate. Type II (MB coursing anterior to the palatal spine) was identified in 23.75% of patients. Type III was present in 11.25%, The mean diameter of the GPA was 0.99 ± 0.16 mm, while the DPA was significantly larger in males ($p = 0.036$). The GPA's lateral branch narrowed anteriorly, with the smallest mucosal-to-vessel distance measured at the first premolar region (2.55 ± 1.11 mm), indicating a heightened risk for surgical injury. No significant relationship was found between palatal vault morphology and mucosal thickness.

Conclusion The LPA contributed to medial hard palate perfusion in the absence of the GPA's medial branch, indicating its surgical relevance in mucogingival procedures.

Keywords Palatine artery · Three-dimensional imaging · Palatal mucosa · Periodontal surgical procedures · Mucogingival surgery · Angiography

Introduction

The palatal mucosa has been widely utilised as an autogenous donor site for subepithelial connective tissue and free gingival grafts (FGG) in mucogingival surgical procedures, particularly for the management of soft tissue deficiencies around teeth and dental implants [13, 16]. Harvesting of FGG is commonly performed from the region extending from the distal aspect of the maxillary canine to the midpalatal area of the first molar [21]. Morphological differences in this region significantly influence the size of the graft that can be obtained [29]. The primary morphological constraints include the limited thickness of the mucosa and the proximity of vital vascular structures, both posing challenges and increasing the risk of surgical complications. [4, 14].

✉ Ahmet Aydogdu
ahm0067@gmail.com

Evrim Bozay Oz
evrimbozay@gmail.com

Ibrahim Ilker Oz
ilkeroz@yahoo.com

[1] Department of Periodontology, Faculty of Dentistry, İstanbul Galata University, Evliya Çelebi Mahallesi Meşrutiyet Caddesi No: 62, Tepebaşı, Beyoğlu, 34430 İstanbul, Turkey

[2] Department of Anaesthesiology and Reanimation, Faculty of Dentistry, Marmara University, 9/3 Maltepe, Başıbüyük Yolu, 34854 İstanbul, Turkey

[3] Department of Radiology, Kartal Dr. Lutfi Kirdar City Hospital, Cevizli Mah. D-100 Güney Yanyol, Cevizli, Kartal, 34865 İstanbul, Turkey

Published online: 14 August 2025

Among these complications, injury to the greater palatine artery (GPA) is the most critical, frequently leading to severe haemorrhage [1, 22]. The GPA, a terminal branch of the descending palatine artery (DPA), originates from the maxillary artery (MA) [11]. Additionally, the lesser palatine artery (LPA), arising as a side branch of the DPA, has been demonstrated in cadaveric studies to predominantly supply the soft palate, while the GPA primarily nourishes the hard palate [2, 3, 17]. Studies revealed significant variability in LPA branching and potential anastomoses with GPA after passing through the greater palatine foramen (GPF) [2, 12, 15]. However, due to inherent challenges associated with the dissection of the pterygopalatine canal (PPC) in cadaveric studies and non-contrast radiological studies, precise branching of vascular structure within this canal remains difficult to ascertain. The studies on the vascularization of the palatal mucosa are limited, with only two significant studies investigating vascular structures within the PPC through cadaveric and radiological analyses [2, 25]. On the other hand, Recent cadaveric investigations using advanced anatomical methods, including latex milk injection and corrosion casting, have enhanced our understanding of the hard palate's vascular architecture. Shahbazi et al. demonstrated complex anastomotic patterns between the GPA, LPA, and nasopalatine artery (NPA), with distinct intraosseous and extraosseous contributions that vary depending on anatomical region and presence of cleft deformities [17, 18]. English-language literature generally accepts that the primary vascular supply to the palatal mucosa is derived from branches of the GPA, yet anatomical differences involving the LPA have not been adequately explored. Understanding the location and depth of the GPA and its branches is essential for minimizing surgical complications such as excessive bleeding, hematoma, paresthesia, and flap necrosis. Complications commonly encountered during or after subepithelial connective tissue graft (SCTG) harvesting include hemorrhage, dehiscence, infection, and discomfort—particularly when fibromucosa thickness is limited or harvesting is too deep [6, 22].Consequently, classifications regarding the vascularization of the palatal mucosa may be incomplete or imprecise, potentially affecting clinical applications in periodontal and implant surgery.

Several radiological studies utilising cone beam computed tomography (CBCT) have evaluated the anatomical features of the GPA, and the greater palatine canal (GPC) or the PPC [7, 23, 28]. Although CBCT provides valuable anatomical information about bone structures, a principal limitation is the inability to distinctly differentiate vascular structures from adjacent tissues due to the absence of contrast enhancement [22, 28]. This technical constraint significantly impairs the accurate identification of vascular structures traversing foramina and canals of the hard palate.

To overcome these limitations, the present study utilises three-dimensional rotational angiography (3D-RA), an advanced imaging technique that allows for simultaneous acquisition of high-resolution, thin-section CBCT images during conventional angiography. By integrating advantages of both traditional angiography and CBCT, this method facilitates detailed visualisation of vascular structures in three dimensions, enabling a more precise assessment of anatomical relationships within the PPC.

The aim of this study is to provide a comprehensive understanding of the vascularization of the palatal mucosa and to investigate potential associations between vascular structures and anatomical features of the maxillary region. Furthermore, this study seeks to elucidate branching patterns of the LPA within the PPC. By offering a more precise vascular mapping of the palatal region, findings from this study are expected to contribute to improved surgical planning and enhanced safety in periodontal and mucogingival procedures, ultimately reducing the risk of vascular complications during graft harvesting.

Materials and methods

Study sample

This retrospective study was approved by the institutional ethics committee (E-54022451-050.05.04-22084), and written informed consent was obtained from all participants. Between June 2020 and May 2021, all consecutive adult patients who underwent cerebral or carotid artery digital subtraction angiography (DSA) with unilateral or bilateral 3D-RA via common carotid artery injection were included. Patients under 18 years, those presenting with dentofacial deformities, and individuals with external carotid artery stenosis exceeding 70% or total occlusion were excluded from the study. Furthermore, patients whose imaging quality was compromised due to motion artefacts, rendering optimisation unfeasible, were also excluded. Retrospective analysis using 3D-RA images was performed on 80 patients to evaluate DPA and its branches, palatal vault morphology, and mucosal thickness. Five patients were excluded due to inadequate image quality. The checklist and reporting standards for anatomical variations defined by Wysiadecki et al. were utilised to ensure the standardisation of this study [27]. The greater and lesser palatine arteries were reviewed in Bergman's Comprehensive Encyclopaedia of Human Anatomical Variation; however, no specific descriptions regarding their anatomical variations were identified [26].

3D-RA and CBCT imaging protocols

All imaging was performed at a single institution and the same imaging platform using a monoplane flat-panel angiography system (Allura Xper FD20, Philips Medical Systems, the Netherlands) with a standardised acquisition and reconstruction protocol (the Cerebral Prop Scan acquisition protocol) under default manufacturer settings. Raw data were acquired with a diagnostic catheter placed in the common carotid artery. A contrast medium (300 mg I/mL) was injected at a rate of 4 mL/s for 6 s (total volume: 24 mL) with a 2-s imaging delay.

Post-processing of the raw data was conducted using Allura 3D-RA 6.4.6 and XperCT Dual 3.2.6 (Philips Medical Systems, Netherlands) on a workstation. High-resolution CBCT reconstructions were generated with a slice thickness ranging from 0.14 to 0.36 mm, enabling detailed visualisation of vascular structures.

Image analysis

CBCT image analysis was performed in consensus by a radiologist and a periodontologist using Allura 3D-RA 6.4.6 on a dedicated workstation. Image manipulation was permitted to enhance visualisation of vascular structures and optimise morphological assessments. Arterial structures were evaluated using maximum intensity projection (MIP) images with a slice thickness of 10–20 mm.

For standardisation, measurements were performed on multiplanar reconstruction (MPR) images (Fig. 1), using consistent anatomical landmarks:

- *Axial images:* A reference line was drawn parallel to the incisive fossa and posterior nasal spine.
- *Sagittal images:* A second reference line was positioned parallel to the nasal floor.
- *Coronal images:* A third line was aligned parallel to the hard palate.

Diameters of the DPA and LPA were measured on sagittal reformatted images at the level of the PPC. The GPA diameter was assessed on coronal reformatted images at the level of the GPF, following previously established methods [8]. The labial branch of the GPA, its terminal branch, was measured at the levels of the first and second molars and premolars. The medial and lateral branches of the GPA were evaluated at the level of the palatal spine. Based on previous studies, the branching pattern of the GPA and the arterial supply of the hard palate were analysed.

Palatal morphology and mucosal thickness measurements

Palatal width and depth were assessed using coronal reformatted images, with modifications based on the descriptions by Klosek et al. [10]. The palatal width (PW7) was defined as the distance between the alveolar bone crests of the maxillary second molars. The GPF-A distance was measured from the centre of the GPF to the median sagittal plane.

For vertical measurements, the reference point was the alveolar bone crest at the level of the maxillary first premolar and second molar:

- *Total palatal vault depth (TPVD):* Measured vertically from the alveolar crest to the palatal sagittal midline.
- *Greater palatine sulcus rim depth (GPSRD):* Measured from the alveolar crest to the external rim of the sulcus.
- *Greater palatine sulcus alveolar slope depth (GPSRAS):* Measured along the slope of the maxillary alveolar process.
- *Greater palatine sulcus vault depth (GPSVD):* Measured vertically to the deepest point of the sulcus.

Mucosal thickness was assessed on coronal images at multiple distances from the gingival margin (Fig. 2):

- 3 mm from the gingival margin
- 6 mm from the gingival margin

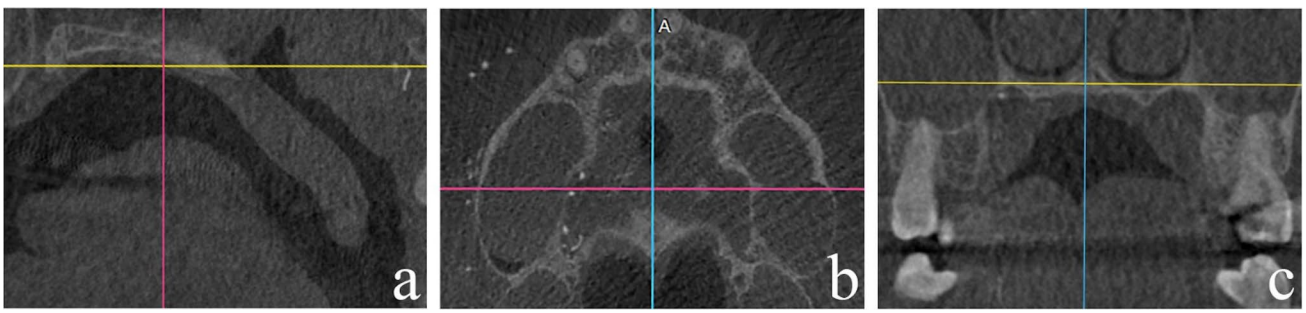

Fig. 1 Multi-planar maximum intensity projection reconstruction used for anatomical standardization. **a** Axial images: a reference line was drawn parallel to the incisive foramen and posterior nasal spine. **b** Sagittal images: a second reference line was aligned parallel to the nasal floor. **c** Coronal images: a third line was set parallel to the hard palate

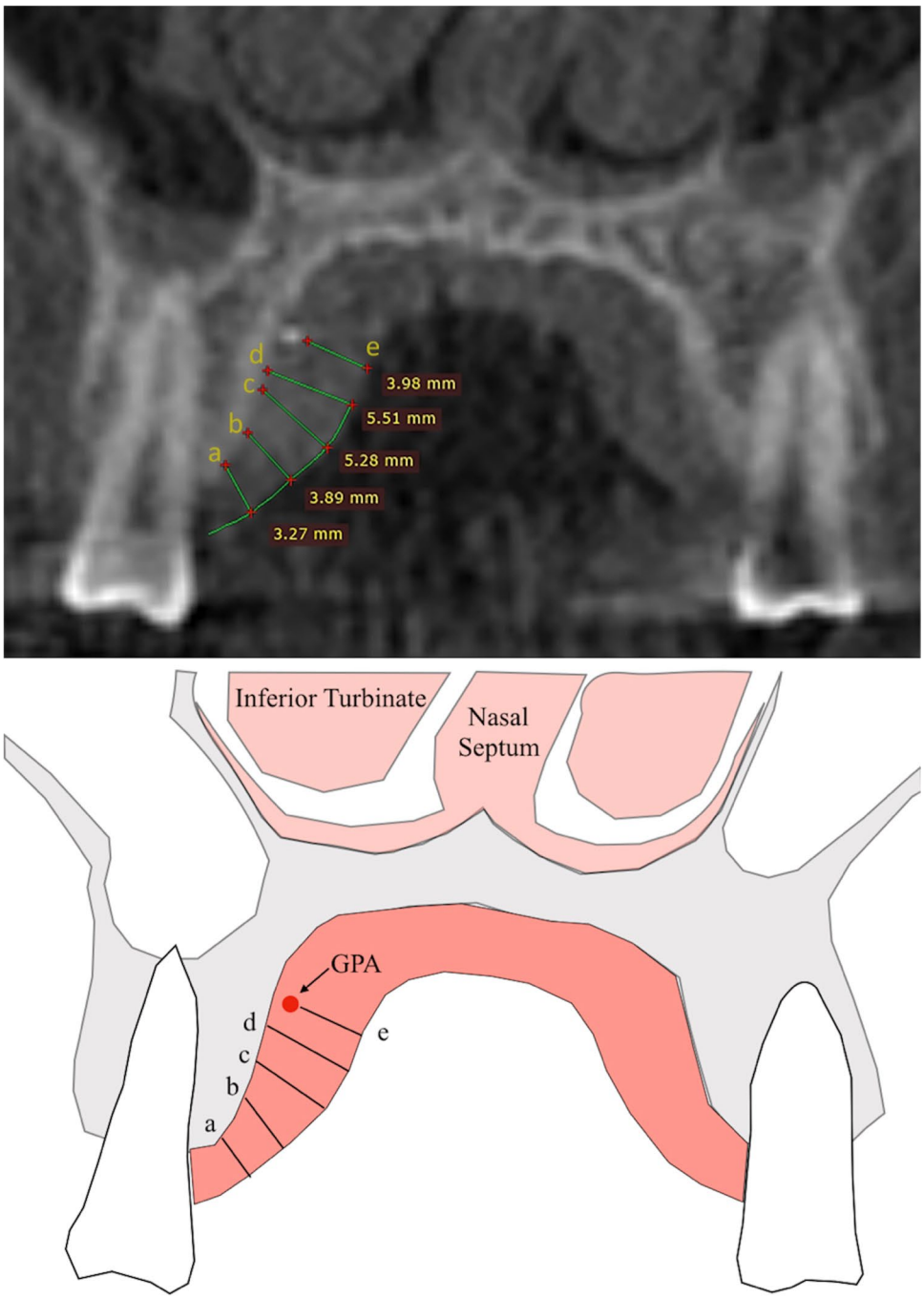

Fig. 2 On the coronal reformatted image and its schematic drawing, mucosal thickness was assessed at multiple distances from the gingival margin, measured at 3-mm intervals **a**–**d** and mucosal thickness was measured between the greater palatine artery (GPA) and the gingival margin

- 9 mm from the gingival margin
- 12 mm from the gingival margin
- Distance from the mucosa to the GPA

Statistical analysis

All statistical analyses were performed using IBM SPSS Statistics for Windows, version 21.0 (IBM Corp., Armonk, NY, USA). The Shapiro–Wilk test was used to assess the normality of continuous variables. For variables with a normal distribution, comparisons between two independent groups were conducted using the independent samples t-test. For non-normally distributed variables, the Kruskal–Wallis test was employed. When significant, post-hoc analyses were carried out using Bonferroni-adjusted Mann–Whitney U tests to control for multiple comparisons. Correlations between palatal vault measurements and mucosal thickness values were evaluated using Spearman's rank correlation analysis. Descriptive statistics are presented as mean ± standard deviation (SD) for normally distributed data and as

median (minimum–maximum) for non-normally distributed data. A *p*-value less than 0.05 was considered statistically significant.

Results

Demographic findings

A total of 80 consecutive patients (24 males and 56 females; mean age: 50.63 ± 13.53 years) meeting the inclusion criteria were included in the study. Measurements were conducted regardless of dental status (dentate or edentulous). Of the participants, 72 had at least three teeth in the molar-premolar area, and eight were completely edentulous.

Arterial measurements and morphological findings

In all cases, the GPA gave rise to the lateral branch (LB) as the terminal branch. The mean GPA diameter was 0.99 ± 0.16 mm, with no statistically significant difference between genders (male: 1.04 ± 0.15 mm, female: 0.97 ± 0.16 mm; $p = 0.089$). The LB was the dominant trunk of the GPA and exhibited the largest diameter at all measured levels (0.87 ± 0.14 mm). However, LB progressively narrowed anteriorly, reaching its smallest diameter (0.52 ± 0.09 mm) at the canine region. MB was found in 28/80 (35%) of the patients, and there were no statistically significant gender differences in LB and MB ($p > 0.05$; Table 1). However, measurements of the DPA at the PPC level revealed a statistically significant difference between genders ($p = 0.036$). Findings related to the LPA are also presented in Table 1.

The GPA branching pattern was classified into three types based on the course of the medial branch (MB) (Fig. 3):

- Type I: No MB arises from the GPA.
- Type II: The MB of the GPA courses anterior to the palatal spine.
- Type III: The MB courses posterior to the palatal spine.

The most prevalent branching pattern was Type I, observed in 52 patients (65%), all of whom exhibited one or more LPA branches supplying the hard palate. Type II, characterised by the MB coursing anterior to the palatal spine, was identified in 19 patients (23.75%). Type III was present in 9 patients (11.25%), and they have at least one LPA branch supplying the hard palate. In five patients (6.25%), LPA was not observed; in all of these cases, the MB was present and originated anteriorly. In all remaining patients, at least one LPA contributed to the vascularization of the hard palate.

Table 1 Distrubiton of arterial vessel diameters (mm) among gender

Gender		AGE	DPA	LPA	GPA	proxLB	proxMB	proxCB	LB at M2	LB at M1	LB at P2	LB at P1	LB at C
N = 24 Male	Median	53.50	1.28	0.78	1.05	0.89	0.68	0.76	0.91	0.97	0.88	0.80	0.54
	Minimum	33.00	0.90	0.52	0.67	0.74	0.51	0.74	0.61	0.65	0.59	0.53	0.36
	Maximum	76.00	1.60	1.06	1.32	1.22	0.84	0.99	1.13	1.20	1.10	0.99	0.66
N = 56 Female	Median	51.00	1.18	0.85	0.97	0.85	0.74	0.73	0.83	0.88	0.81	0.73	0.49
	Minimum	18.00	0.72	0.45	0.65	0.50	0.50	0.49	0.60	0.64	0.58	0.53	0.35
	Maximum	77.00	1.60	1.23	1.30	1.14	0.90	0.89	1.20	1.28	1.17	1.06	0.70
	P values	0.428	0.012	0.884	0.083	0.285	0.349	0.237	0.289	0.302	0.387	0.361	0.155
N = 80 Total	Median	51.00	1.21	0.84	1.00	0.86	0.74	0.74	0.87	0.92	0.85	0.77	0.52
	Minimum	18.00	0.72	0.45	0.65	0.50	0.50	0.49	0.60	0.64	0.58	0.53	0.35
	Maximum	77.00	1.60	1.23	1.32	1.22	0.90	0.99	1.20	1.28	1.17	1.06	0.70

Values were given as Median, minimum, maximum, prox: proxmial of artery that was measured the diameter. DPA: Descenden Palatine Artery; LPA: Lesser Palatine Artery; GPA: Greater Palatine Artery; LB: Lateral Branch; MB: Medial Branch; CB: Canin Branch; M2: Second molar region; M1: First Molar Region; P2: Second premolar region; P1: First Premolar region; C: Canin region Mann Whitney U test was performed

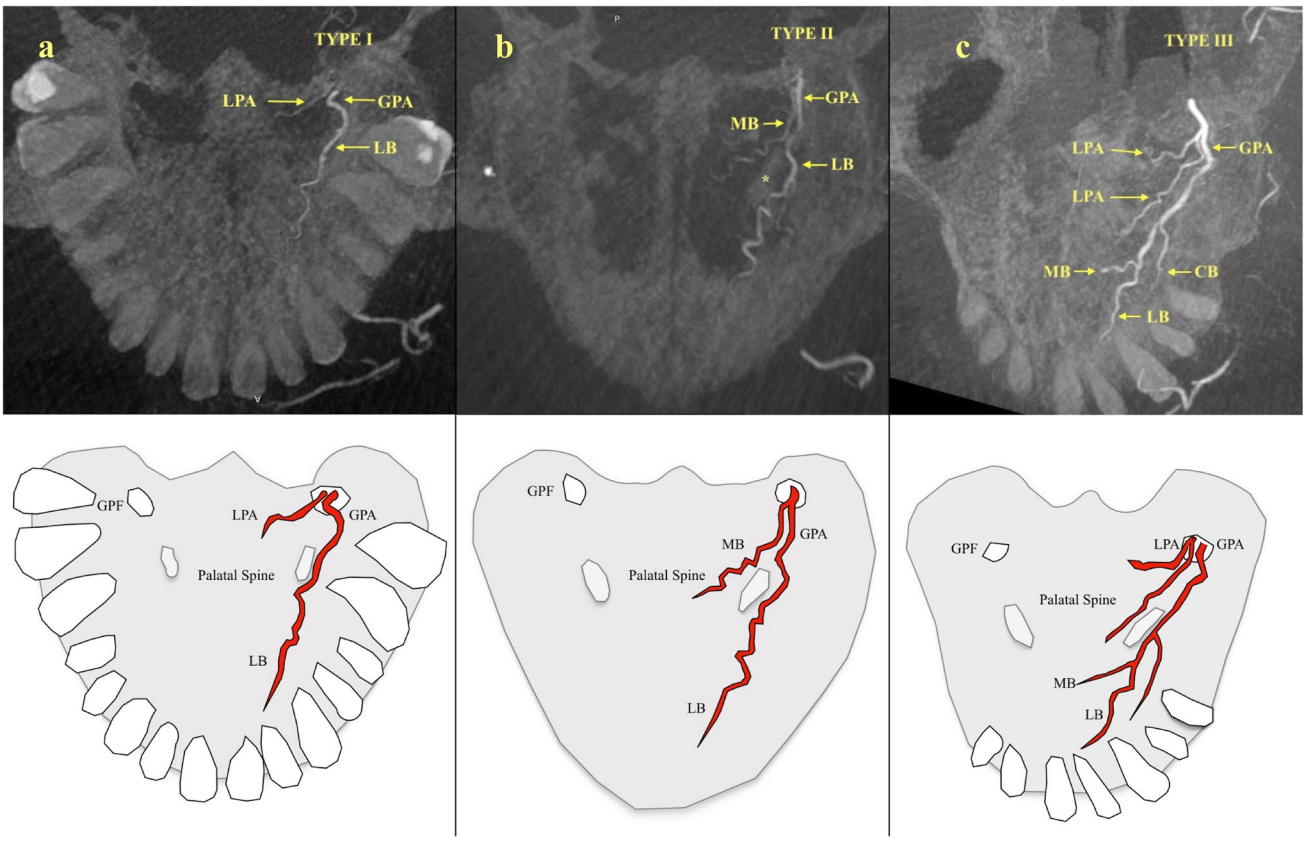

Fig. 3 The branching pattern of the greater palatine artery (GPA) was classified into three types based on the course of the medial branch (MB): Type I, in which no MB arises from the GPA (**a**) Type II, in which the medial branch courses anterior to the palatal spine* (**b**) and Type III, in which the MB courses posterior to the palatal spine* (**c**) on the axial reformatted images and their schematic drawings. (LPA: lesser palatine artery, LB: lateral branch, CB: canine branch)

According to the finding of the GPA's branching pattern, the vascularization of the hard palate was classified based on the contributions of the LPA:

- Type I: one or more LPA contributing to hard palate vascularization (75/80, 93.75%).
- Type II: no LPA contribution to the hard palate vascularization (5/80, 6.25%.

Palatal vault measurements

The median TPVD was 39.26 mm. Although male patients exhibited a wider vault (40.97 mm) compared to female patients (38.34 mm), the gender difference was not statistically significant ($p=0.186$, $p=0.869$). Other palatal vault measurements are provided in Table 3, with no statistically significant gender differences observed.

Mucosal findings

The thickness of the palatal mucosa was assessed at five dental levels (M2, M1, P2, P1, C) and at four measurement points (a–d) extending 3 mm from the radiological gingival margin. A gradual increase in mucosal thickness was observed from coronal to apical regions, with the thickest mucosa at the maxillary first molar (M1) and the thinnest at the first premolar (P1) (Table 2).

The distance between the palatal mucosa and the LB of the GPA was greatest at the M1 level (5.68 ± 2.53 mm), whereas the shortest distance was recorded at the P1 level (2.55 ± 1.11 mm) (Table 3).

There were no statistically significant gender differences in palatal mucosal thickness. However, in general, female patients exhibited thicker palatal mucosa across all measurement points, except for the palatal midline mucosa (PMM), though these differences were not statistically significant. The PMM was found to be thicker from the canine to the P1 in male patients, whereas it was thicker from the second premolar (P2) to the P2 in female patients, although this trend was not statistically significant (Table 3). No significant correlations were found between palatal vault measurements and mucosal thickness (Table 4).

Table 2 Distrubiton of radiological mucosal tickness (mm) of hard palate among genders

Gender		M2a	M2b	M2c	M2d	M1a	M1b	M1c	M1d	P2a	P2b	P2c	P2d	P1a	P1b	P1c	P1d	Ca	Cb	Cc	Cd
N = 24 Male	Median	1.74	2.19	2.86	4.07	1.64	2.04	2.99	4.67	2.02	2.70	3.02	3.47	1.76	2.21	2.52	2.80	2.21	2.72	3.27	3.15
	Min	0.70	1.63	1.92	2.80	0.66	0.82	1.20	1.89	0.81	1.08	1.21	1.39	0.66	0.84	0.96	1.08	0.89	1.11	1.31	1.26
	Max	5.10	5.03	6.18	6.54	4.80	5.77	8.76	13.84	5.93	7.91	8.86	10.17	5.29	6.61	7.52	8.35	6.48	7.98	9.57	9.22
N = 56 Female	Median	2.04	2.56	3.06	4.17	1.92	2.39	3.50	5.40	2.37	3.16	3.54	4.07	2.07	2.60	2.96	3.29	2.59	3.19	3.83	3.69
	Min	1.00	1.58	1.54	2.92	0.94	1.17	1.72	2.71	1.16	1.55	1.74	1.99	0.98	1.24	1.41	1.58	1.27	1.56	1.88	1.81
	Max	5.03	5.71	6.74	8.92	4.73	5.79	8.64	13.65	5.84	7.80	8.74	10.03	5.22	6.52	7.42	8.23	6.39	7.87	9.44	9.09
	P value	0.286	0.470	0.859	0.107	0.117	0.133	0.231	0.325	0.178	0.143	0.112	0.288	0.412	0.336	0.177	0.630	0.098	0.393	0.512	0.489
N = 80 Total	Median	1.97	2.53	2.93	4.16	1.85	2.30	3.38	5.24	2.28	3.05	3.41	3.92	1.99	2.50	2.85	3.17	2.50	3.07	3.63	3.55
	Min	0.70	1.58	1.54	2.80	0.66	0.82	1.20	1.89	0.81	1.08	1.21	1.39	0.66	0.84	0.96	1.08	0.89	1.11	1.31	1.26
	Max	5.10	5.71	6.74	8.92	4.80	5.79	8.76	13.84	5.93	7.91	8.86	10.17	5.29	6.61	7.52	8.35	6.48	7.98	9.57	9.22

Values were given as Median. minimum (min). maximum (max) M2: Second molar region; M1: First Molar Region; P2: Second premolar region; P1: First Premolar region; C: Canin region
a:mucosal thickness at 3 mm from gingival margin; b: thickness at 6 mm from gingival margin; c: thickness at 9 mm from gingival margin; d: thickness at 12 mm from gingival margin

Discussion

Arterial measurements and morphological findings

After emerging from the GPF, the terminal branch of the DPA is known as the GPA. The LPA demonstrates greater variability regarding its origin and branching. A recent meta-analysis by Kim et al., evaluating 75 studies comprising 22,202 specimens, focused on the anatomy of the GPF and PPC in relation to the GPA but primarily relied on morphometric or imaging data without detailed vascular anatomical information regarding the course, branching pattern, or variability of the GPA and LPA [9]. In the aforementioned ultrasonographic study involving 31 healthy individuals, the location of the GPF, course of the GPA, collateral branches, and palatal fibromucosa thickness were successfully assessed using intraoral ultrasonography; however, similar to other non-invasive imaging modalities, this study did not evaluate the presence or anatomical contribution of the LPA, thus limiting its utility in comprehensively mapping palatal vascularization [24]. Moreover, the number of studies simultaneously evaluating both GPA and LPA is very limited, and radiological assessments pertaining to this matter are conspicuously lacking in the English medical literature [17, 29]. Yu et al. classified all arterial structures arising from the GPF as GPA and its branches [29]. However, this approach did not account for the role of LPA in hard palate vascularization or the morphological diversity of GPA branching. Although Shahbazi et al. demonstrated the contribution of the LPA to the maxillary tuberosity through anastomotic branches in a cadaveric model, their study did not evaluate its intraforaminal course or direct contribution to the vascularization of the hard palate, which contrasts with the 3D-RA-based findings where multiple LPA branches originating within the PPC were shown to significantly supply the medial palatal mucosa [17]. Similarly, the literature review by Tavelli et al. did not evaluate GPA and LPA variations concurrently [22]. In this analysis, GPA branching patterns and hard palate vascularization were described separately, offering anatomical data useful for reducing vascular complications during mucogingival procedures.

This study provides a revised classification of GPA branching patterns and offers a comprehensive categorization of the arterial supply to the hard palate. It revealed that in 76.25% of cases, GPA and LPA originated simultaneously from the GPF (Fig. 4). Additionally, at least one LPA branch contributed to medial hard palate perfusion in 93.75% of the cases. GPA was categorized into three types based on the presence and course of the medial branch (MB), with Type I (no MB present) being the most frequent (65%). This differs from the findings of Yu et al., who reported frequent identification of a distinct MB originating from the lateral branch (LB) either posterior (41.7%) or anterior (33.3%) to the palatal spine. The discrepancy might be due to Yu et al.'s potential misinterpretation of some LPA

Table 3 Distribuiton of palatal vault measurement (mm) among genders

Gender		PW7	GPSRD	GPSVD	GPSRAS	GPF	LENGHT	WIDTH	RATIO	Ma2	Ma1	Pa2	Pa1	Ca
N=24 Male	Median	19.77	8.39	11.98	8.48	14.88	40.97	13.46	3.14	5.75	4.78	2.55	2.11	3.13
	Min	14.90	2.51	5.22	2.96	11.98	36.59	5.78	2.19	3.75	1.92	1.02	0.85	1.22
	Max	24.36	14.31	16.36	13.52	18.72	49.68	18.21	6.14	9.16	14.05	7.46	6.18	9.12
N=56 Female	Median	19.17	8.27	11.33	8.93	14.40	38.34	11.93	3.10	4.75	5.52	2.98	2.53	3.81
	Min	15.68	2.74	6.40	3.25	9.89	33.18	5.34	1.86	2.72	2.75	1.46	1.21	1.80
	Max	25.93	17.18	16.35	12.67	17.66	47.12	17.80	7.72	11.04	13.86	7.36	6.10	9.08
N=80 Total	Median	19.46	8.29	11.41	8.93	14.48	39.26	12.61	3.13	4.81	5.33	2.88	2.41	3.75
	Min	14.90	2.51	5.22	2.96	9.89	33.18	5.34	1.86	2.72	1.92	1.02	0.85	1.29
	Max	25.93	17.18	16.36	13.52	18.72	49.68	18.21	7.72	11.04	14.05	7.46	6.18	9.20

Values were given as Median. minimum (min). maximum (max) PW7: PalataL width at 2. Molar region; GPSRD:; GPSVD:;GPSRAS:; GPF:; LENGHT:; WIDTH:; RATIO: Ma2: distance from mucosa to artery at second molar region; Ma1:: distance from mucosa to artery First Molar Region; Pa2: distance from mucosa to artery Second premolar region; Pa1:: distance from mucosa to artery First Premolar region; Ca: distance from mucosa to artery Canin region

branches as medial branches of the GPA. These results clarify that when an MB is absent, the LPA notably contributes to hard palate vascularization, supporting our interpretation of previous findings by Yu et al. [29].

Griffin et al. reported lower necrosis rates in the palatal region than in the upper first molar and premolar regions, where vascular injury risk was 5.7% [5]. Anastomoses between the GPA, anterior palatine artery, nasopalatine artery, and LPA likely provide vascular redundancy that reduces necrosis risk. This anatomical framework supports future research exploring whether submucosal anaesthetic injections at contralateral palatal foramina reduce intraoperative bleeding during graft harvesting or sinus lift procedures. Newly identified contralateral anastomoses suggest that bilateral connective tissue grafting may impair palatal blood supply and increase necrosis risk.

GPA measurements in this study align with findings from Kim et al. who used intra-arterial latex injections [8]. Klosek et al. reported larger GPA diameters, possibly because latex coating was not applied [10]. No studies have used contrast-enhanced radiology to measure GPA diameters. Radiological imaging in living subjects could improve accuracy in submillimeter measurements compared to cadaver studies.

Mucosal findings

Palatal mucosal thickness was measured from the radiological gingival margin. This was preferred over the cementoenamel junction to avoid errors in edentulous cases or those with gingival recession. Mucosal thickness values were similar to those reported by Kim et al. based on sectional palatal images [8]. Compared to Song et al., the measurements were higher; that may be attributed to the reduced spatial resolution caused by the 2 mm slice thickness used in the 512×512 matrix, which reduces edge sharpness and inflates measurements [20]. Mucosal thickness and the distance between the mucosal surface and vascular structures directly affect graft survival. Grafts must allow adequate nutrient diffusion without increasing necrosis or vascular injury risk. Literature recommends a graft thickness between 1.0 and 1.5 mm [20]. Excessive thickness reduces integration potential, while thin grafts risk necrosis. Tavelli et al. described a “safety zone” width ranging from 10.9 mm in molars to 5 mm in the canine region [22]. Zucchelli et al. reported mean graft thicknesses of 1.34±0.26 mm and 1.32±0.16 mm; however, primary flap necrosis occurred in 28% of the test group during the first week [30]. This study found 29% of mucosal thickness measurements below the 1.5 mm threshold, suggesting higher vascular injury risk. LB passed closest to the mucosa at the first premolar level, differing from findings by Kim et al. [8]. This discrepancy may be attributed to reduced spatial resolution caused by increased section thickness. Average LB-to-mucosa distance at this

Table 4 Correlation matrix among palatal vault measurements and palatal mucosa thiknesses

	WIDTH	RATIO	PW7	GPSRD	GPSVD	GPSRAS	GPF	M2	M1	P2	P1	C
LENGTH	0.089	0.356**	0.826**	−0.076	0.083	−0.019	0.490**	0.095	0.116	0.125	0.133	0.142
WIDTH		0.865**	−0.038	0.571**	0.793**	0.581**	−0.177	0.126	−0.066	−0.084	−0.090	−0.093
RATIO			0.393**	0.537**	0.718**	−0.522**	0.427**	−0.002	0.190	0.197	0.210	0.368
PW7				−0.245*	0.047	−0.119	0.596**	0.034	0.012	0.023	0.025	0.306
GPSRD					0.347**	0.851**	−0.320**	0.080	0.023	0.013	0.014	0.441
GPSVD						0.547**	−0.177	0.047	0.014	0.001	0.025	0.063
GPSRAS							−0.346**	0.169	0.109	0.083	0.096	0.094
GPF								−0.219	−0.309*	−0.291	−0.311	−0.381
M2									0.642**	0.637**	0.679**	0.724**
M1										0.875**	0.757**	0.807**
P2											0.572**	0.930**
P1												0.757**

Sperman Correlation was performed **Correlation is significant at the 0.01 level (2-tailed). *Correlation is significant at the 0.05 level (2-tailed)

level was 2.55 mm, with the closest measurement recorded at 0.85 mm.

The increased use of palatal mini-screw anchorage in orthodontics raises concern about vascular injury. Palatal arteries are also at risk during cleft repair, maxillary surgeries, and orthognathic procedures. In situations where collateral circulation is limited, palatal artery injury could cause significant complications. Insufficient mucosal thickness increases risks of necrosis, delayed healing, and postoperative pain. Damage to blood vessels during incision heightens these risks. Necrosis of palatal mucosa and hard tissue is possible. GPA, along with labial and canine branches, plays a central role in palatal blood supply.

No correlation was observed between bony prominence and GPA branching patterns, confirming Yu et al.'s findings [29]. Palatal vault measurements matched previous studies, showing no relationship with GPA morphology. These observations suggest that predicting vascular injury in the hard palate based solely on topographic data remains unreliable.

When compared with recent cadaveric investigations, Shahbazi et al. demonstrated the presence of intraosseous horizontal and vertico-oblique anastomoses between the GPA, posterior superior alveolar artery, and infraorbital artery within the maxilla, emphasizing the risk of ischemic complications when these vascular loops are compromised [19]. Subsequently, Shahbazi et al. reported that in cases of cleft palate, the collateral circulation is altered, particularly with a reduction in midline and intraosseous GPA anastomoses, highlighting the importance of preserving the remaining vascular networks during surgical interventions [18]. In contrast, the present 3D-RA study revealed that the LPA significantly contributes to the perfusion of the medial hard palate, particularly in GPA Type I configurations where the medial branch is absent. This finding underscores the necessity of accounting for both arteries in surgical planning. Moreover, the shortest mucosal-to-GPA distance was identified in the premolar region, correlating with previously established high-risk zones for vascular injury during palatal graft harvesting.

This research possesses some limitations. The included patients were those receiving cerebral or carotid angiography, potentially resulting in selection bias. Consequently, the results may not accurately represent the homogeneous demographic distribution. Additionally obtaining substantial sample sizes, as demonstrated in traditional imaging investigations, is impractical in the short to medium term owing to the invasive characteristics of the 3D-RA. While edentulous patients were included, the influence of dentition status on palatal artery anatomy and mucosal thickness was not evaluated independently.

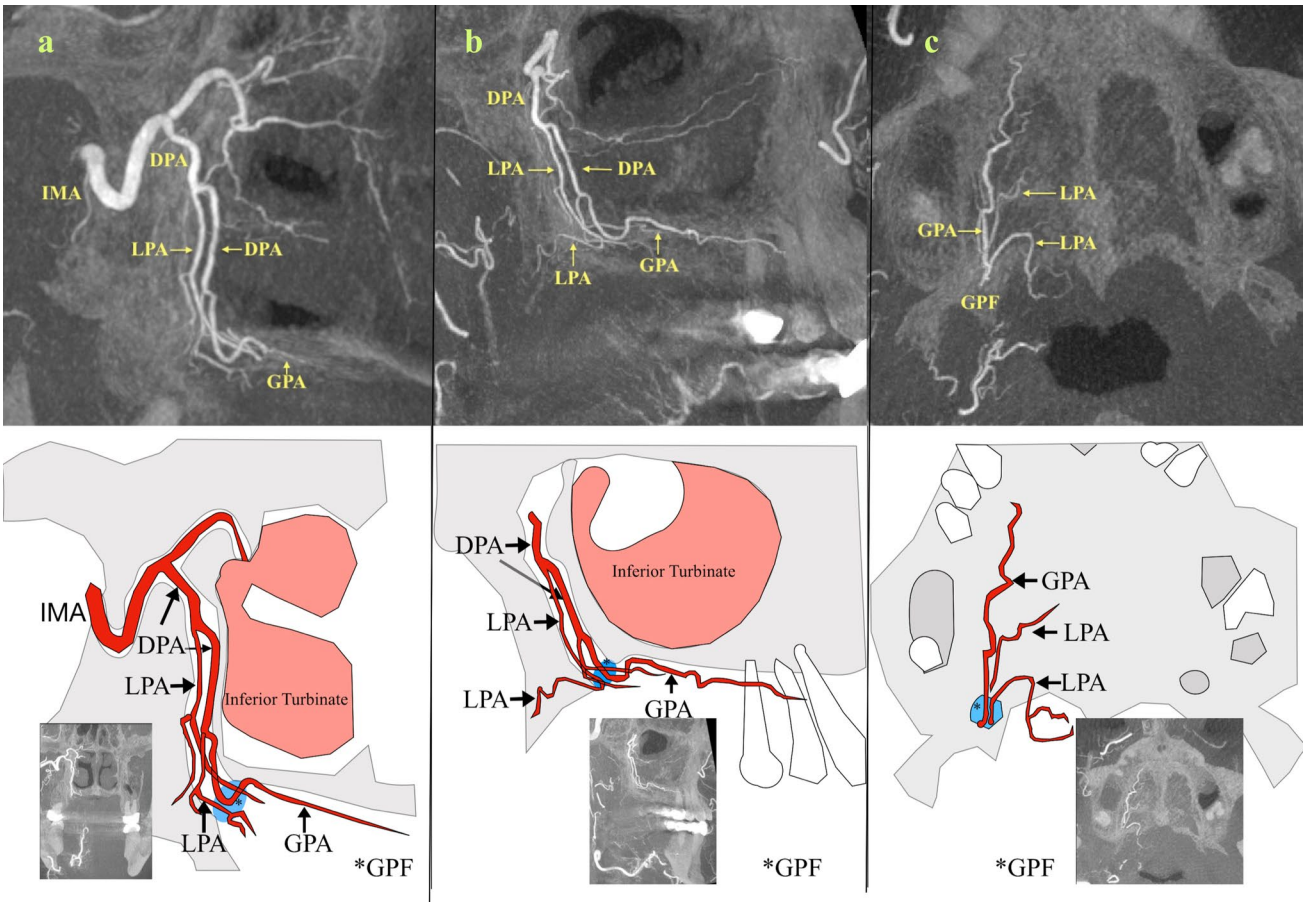

Fig. 4 Coronal (**a**) sagittal (**b**) and axial (**c**) maximum intensity projection reconstruction images and their schematic drawings demonstrating the simultaneous origin of one greater palatine artery (GPA) and multiple Lesser Palatine Arteries (LPAs) from the greater palatine foramen (GPF). Additionally, multiple LPAs are observed arising as side branches from the descending palatine artery (DPA) within the greater palatine canal. (IMA: internal maxillary artery)

Conclusion

This study refines GPA classifications, underscores the LPA's role in palatal vascularization, and highlights variability in mucosal thickness and vascular proximity. The absence of the MB in the Type I GPA pattern highlighted the compensatory role of the LPA in supplying the medial hard palate, underscoring the clinical importance of preserving the LPA during mucogingival surgery to enhance surgical safety. Continued advancements in imaging technologies are expected to improve anatomical mapping and surgical planning in this complex anatomical region.

Author contributions CRediT author statement Ibrahim Ilker OZ: Conceptualization, Methodology, Writing—Original draft preparation, Writing—Reviewing and Editing. Ahmet Aydogdu: Validation, Data curation, Formal analysis, Software, Writing—Reviewing and Editing. Evrim Bozay Oz: Visualization, Investigation, Resources, Writing- Reviewing and Editing.

Funding None.

Data availability No datasets were generated or analysed during the current study.

Declarations

Competing interests The authors declare no competing interests.

Ethical approval and consent to participate The Bezmialem Vakif University Ethics Committee approved the imaging study (number of approval: E-54022451-050.05.04-22084). The research was conducted ethically, following the Code of Ethics of the World Medical Association (Declaration of Helsinki).

References

1. Brasher WJ, Rees TD, Boyce WA (1975) Complications of free grafts of masticatory mucosa. J Periodontol 46(3):133–138. https://doi.org/10.1902/jop.1975.46.3.133
2. Choi J, Park HS (2003) The clinical anatomy of the maxillary artery in the pterygopalatine fossa. J Oral Maxillofac Surg 61(1):72–78. https://doi.org/10.1053/joms.2003.50012
3. Fu JH, Hasso DG, Yeh CY, Leong DJ, Chan HL, Wang HL (2011) The accuracy of identifying the greater palatine neurovascular

bundle: a cadaver study. J Periodontol 82(7):1000–1006. https://doi.org/10.1902/jop.2011.100619
4. Greenstein G, Cavallaro J, Tarnow D (2008) Practical application of anatomy for the dental implant surgeon. J Periodontol 79(10):1833–1846. https://doi.org/10.1902/jop.2008.080086
5. Griffin TJ, Cheung WS, Zavras AI, Damoulis PD (2006) Postoperative complications following gingival augmentation procedures. J Periodontol 77(12):2070–2079. https://doi.org/10.1902/jop.2006.050296
6. Herman L, Font K, Soldatos N, Chandrasekaran S, Powell C (2022) The surgical anatomy of the greater palatine artery: a human cadaver study. Int J Periodontics Restorative Dent 42(2):233–241. https://doi.org/10.11607/prd.4945
7. Ikuta CR, Cardoso CL, Ferreira-Júnior O, Lauris JR, Souza PH, Rubira-Bullen IR (2013) Position of the greater palatine foramen: an anatomical study through cone beam computed tomography images. Surg Radiol Anat 35(9):837–842. https://doi.org/10.1007/s00276-013-1151-z
8. Kim DH, Won SY, Bae JH, Jung UW, Park DS, Kim HJ, Hu KS (2014) Topography of the greater palatine artery and the palatal vault for various types of periodontal plastic surgery. Clin Anat 27(4):578–584. https://doi.org/10.1002/ca.22252
9. Kim DW, Tempski J, Surma J, Ratusznik J, Raputa W, Świerczek I, Pękala JR, Tomaszewska IM (2023) Anatomy of the greater palatine foramen and canal and their clinical significance in relation to the greater palatine artery: a systematic review and meta-analysis. Surg Radiol Anat 45(2):101–119. https://doi.org/10.1007/s00276-022-03061-z
10. Klosek SK, Rungruang T (2009) Anatomical study of the greater palatine artery and related structures of the palatal vault: considerations for palate as the subepithelial connective tissue graft donor site. Surg Radiol Anat 31(4):245–250. https://doi.org/10.1007/s00276-008-0432-4
11. Leo J (2023) The head and neck. In: Leo J (ed) Clinical anatomy and embryology: a guide for the classroom, boards, and clinic. Springer International Publishing, Cham, pp 3–76
12. Li KK, Meara JG, Alexander A Jr (1996) Location of the descending palatine artery in relation to the Le Fort I osteotomy. J Oral Maxillofac Surg 54(7):822–825. https://doi.org/10.1016/s0278-2391(96)90528-5
13. Monnet-Corti V, Santini A, Glise JM, Fouque-Deruelle C, Dillier FL, Liébart MF, Borghetti A (2006) Connective tissue graft for gingival recession treatment: assessment of the maximum graft dimensions at the palatal vault as a donor site. J Periodontol 77(5):899–902. https://doi.org/10.1902/jop.2006.050047
14. Mörmann W, Schaer F, Firestone AR (1981) The relationship between success of free gingival grafts and transplant thickness. Revascularization and shrinkage—a one year clinical study. J Periodontol 52(2):74–80. https://doi.org/10.1902/jop.1981.52.2.74
15. Navarro JA, Filho JL, Zorzetto NL (1982) Anatomy of the maxillary artery into the pterygomaxillopalatine fossa. Anat Anz 152(5):413–433
16. Reiser GM, Bruno JF, Mahan PE, Larkin LH (1996) The subepithelial connective tissue graft palatal donor site: anatomic considerations for surgeons. Int J Periodontics Restor Dent 16(2):130–137
17. Shahbazi A, Grimm A, Feigl G, Gerber G, Székely AD, Molnár B, Windisch P (2019) Analysis of blood supply in the hard palate and maxillary tuberosity-clinical implications for flap design and soft tissue graft harvesting (a human cadaver study). Clin Oral Investig 23(3):1153–1160. https://doi.org/10.1007/s00784-018-2538-3
18. Shahbazi A, Mueller AA, Mezey S, Gschwindt S, Kiss T, Baksa G, Kisnisci RS (2024) Is the collateral circulation pattern in the hard palate affected by cleft deformity? Clin Oral Invest 28(5):277. https://doi.org/10.1007/s00784-024-05627-0
19. Shahbazi A, Sculean A, Baksa G, Gschwindt S, Molnár B, Vág J, Bogdán S (2023) Intraosseous arterial alteration of maxilla influencing implant-related surgeries. Clin Oral Investig 27(9):5217–5221. https://doi.org/10.1007/s00784-023-05141-9
20. Song JE, Um YJ, Kim CS, Choi SH, Cho KS, Kim CK, Chai JK, Jung UW (2008) Thickness of posterior palatal masticatory mucosa: the use of computerized tomography. J Periodontol 79(3):406–412. https://doi.org/10.1902/jop.2008.070302
21. Sullivan HC, Atkins JH (1968) Free autogenous gingival grafts. 3. Utilization of grafts in the treatment of gingival recession. Periodontics 6(4):152–160
22. Tavelli L, Barootchi S, Ravidà A, Oh TJ, Wang HL (2019) What is the safety zone for palatal soft tissue graft harvesting based on the locations of the greater palatine artery and foramen? A systematic review. J Oral Maxillofac Surg 77(2):271.e271-271.e279. https://doi.org/10.1016/j.joms.2018.10.002
23. Tomaszewska IM, Tomaszewski KA, Kmiotek EK, Pena IZ, Urbanik A, Nowakowski M, Walocha JA (2014) Anatomical landmarks for the localization of the greater palatine foramen—a study of 1200 head CTs, 150 dry skulls, systematic review of literature and meta-analysis. J Anat 225(4):419–435. https://doi.org/10.1111/joa.12221
24. Torenek Agirman K, Caglayan F (2025) Identification of the greater palatine foramen, the greater palatine artery, and palatal fibromucosa: a cross-sectional ultrasonographic clinical study. J Stomatol Oral Maxillofac Surg. https://doi.org/10.1016/j.jormas.2025.102228
25. Touré G (2019) Distribution of the maxillary artery in the deep regions of the face and the maxilla: clinical applications. J Plast Reconstr Aesthet Surg 72(6):1020–1024. https://doi.org/10.1016/j.bjps.2019.02.008
26. Tubbs RS, Shoja MM, Loukas M (2016) Bergman's comprehensive encyclopedia of human anatomic variation. Wiley, London
27. Wysiadecki G, Varga I, Klejbor I, Balawender K, Ghosh SK, Clarke E, Koziej M, Bonczar M, Ostrowski P, Żytkowski A (2024) Reporting anatomical variations: should unified standards and protocol (checklist) for anatomical studies and case reports be established? Transl Res Anat 35:100284. https://doi.org/10.1016/j.tria.2024.100284
28. Yilmaz HG, Ayali A (2015) Evaluation of the neurovascular bundle position at the palate with cone beam computed tomography: an observational study. Head Face Med 11:39. https://doi.org/10.1186/s13005-015-0097-2
29. Yu SK, Lee MH, Park BS, Jeon YH, Chung YY, Kim HJ (2014) Topographical relationship of the greater palatine artery and the palatal spine. significance for periodontal surgery. J Clin Periodontol 41(9):908–913. https://doi.org/10.1111/jcpe.12288
30. Zucchelli G, Mele M, Stefanini M, Mazzotti C, Marzadori M, Montebugnoli L, de Sanctis M (2010) Patient morbidity and root coverage outcome after subepithelial connective tissue and de-epithelialized grafts: a comparative randomized-controlled clinical trial. J Clin Periodontol 37(8):728–738. https://doi.org/10.1111/j.1600-051X.2010.01550.x